RADIOELEMENT GEOCHEMISTRY: FIELD EXPERIENCE WITH A ROVER-MOUNTED GAMMA RAY SPECTROMETER. T. H. Prettyman[1], D. T. Vaniman[1], R. C. Clark[1], E. N. Dobrea[1], A. R. Hendrix[1], M. E. Banks[2], M. D. Lane[3], D. S. Wettergreen[4], [1]Planetary Science Institute (prettyman@psi.edu), [2]NASA Goddard Space Flight Center, Greenbelt, MD, [3]Fibernetics LLC, Lititz PA, [4]Carnegie Mellon University, Pittsburgh PA.

Introduction: The elements K, Th, and U include long-lived, primordial radioisotopes (^{40}K, ^{232}Th, and ^{238}U) with distinct gamma ray signatures that can be detected and quantified in situ using a low resource spectrometer (Fig. 1). These natural radioelements have large ionic radii and are incorporated into accessory minerals derived from late-stage magmas. The ratios of the moderately volatile element K to the refractory elements Th and U remain constant during igneous processing. As such, the K/Th ratio of crustal rocks reflects the volatile/refractory ratio of materials that accreted to form the terrestrial planets [e.g., 1].

In aqueous systems, fractionation of K, U, and Th can occur due to differences in their water solubility. Notably, K and U are more soluble in aqueous solutions than Th. As a result, elemental partitioning can occur in various environmental settings (e.g., concentration of Th in ocean sediments or leaching of K and U from surface deposits). Mineral hosts for radioelements include K-feldspars and accessory minerals in granitic rocks as well as phosphate minerals, such as monazite, and phyllosilicates formed by weathering. In clay-bearing terrestrial rocks, the kaolinite-to-illite fraction is sensitive to climate, with higher fractions associated with warmer and wetter environments that favor removal of K and U. As such, the Th/K and Th/U ratios have been proposed as proxies for the clay mineralogy of sedimentary facies [e.g., 2].

Sedimentary rocks, common on Earth's surface, also formed early in the history of Mars within lacustrine and/or marine environments [e.g., 3]. In this abstract we present analyses of analogous materials using data acquired by a rover-mounted Gamma-Ray Spectrometer (GRS). The work was part of a field study carried out in Nov-2021 by the Solar System Exploration Virtual Institute (SSERVI) Toolbox for Exploration (TREX) project [4].

Instrument/Rover: The GRS was a low-cost, low-SWaP (Size, Weight, and Power) instrument used previously to study pyroclastic ash deposits in New Mexico [5]. The sensor was a large (2 kg) bismuth germanate (BGO) scintillator, identical to that flown on Dawn [6], read out by a ruggedized photomultiplier tube. A compact, digital multichannel analyzer and data acquisition computer (DAC) were used to record a time series of gamma ray spectra (Fig. 2). The GRS was mounted to the floor of Carnegie Mellon's Zoë rover [e.g., 7], which provided power to the instrument. Data were uplinked from the field periodically for analysis by

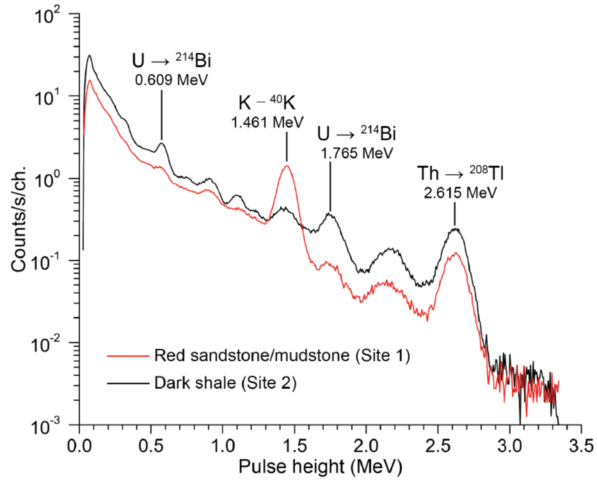

Figure 1. Gamma-ray spectra acquired at field sites in northern Arizona show variability in radioelement content. Key signatures for K, Th, and U are indicated.

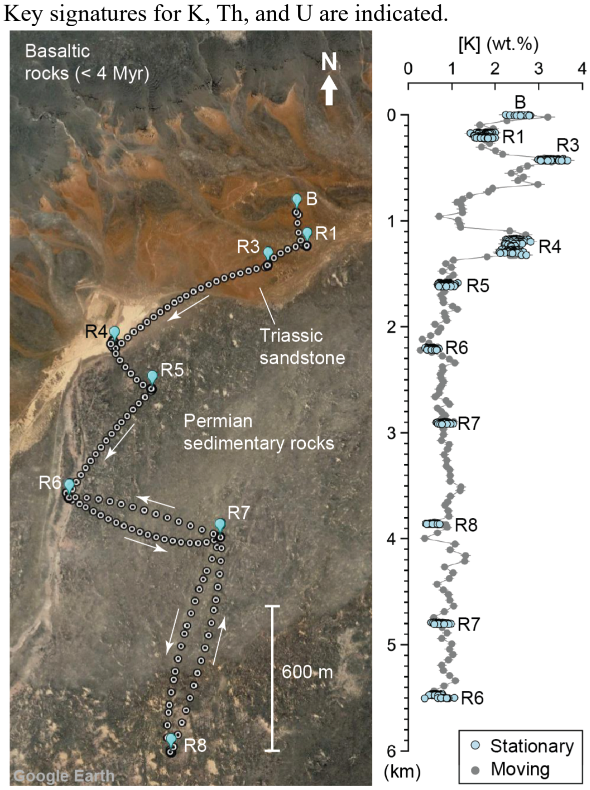

Figure 2. Field Site 1: The path of the rover (circles) and locations where the rover was approximately stationary (blue pins with labels) are shown on the left. The concentration of K along the ~5.5 km traverse from spectra acquired every 70 seconds is shown on the right. Blue circles with labels correspond to the pin locations on the left. The study area, which is bounded to the north by basalts, contains a mixture of sandstone and limestone deposits.

the science team, but were not used in rover autonomous operations. Processing steps included determining measurement locations from rover GPS data (Fig. 2), spectral gain correction, summing of spectra at selected locations, extraction of peak areas, and conversion of counts to elemental concentrations.

Field Sites: The TREX team studied two field sites in northern Arizona containing sedimentary rocks [8]. Site 1 (Fig. 2) was previously mapped as Permian sandstone and limestone deposited in a shallow sea and near-shore environment. Dark red materials to the northwest of the site are likely sandstones and mudstones of the Moenkopi formation. Site 2 contains Cretaceous sediments, including sandstones and shale (Mancos) deposited in a marine environment.

Preliminary Results: Radioelement concentrations along rover traverses at both sites varied considerably between sedimentary facies, but were generally constant within them, consistent with homogeneous deposition of sediments (Fig. 2). Abrupt discontinuities in counts observed when crossing visible boundaries demonstrated approximately meter scale spatial resolution for in situ GRS measurements. The depth sensitivity is known to be a few decimeters. The high efficiency BGO sensor enabled precise measurements of gross gamma counts and radioelements along the traverse and elemental ratios at selected locations (Figs. 2 and 3). Accuracy is primarily limited by uncertainties in decay constants, knowledge of the GRS response function, and assumptions regarding layering. Better than 10% total uncertainty is achievable for the range of elemental concentrations found in sedimentary rocks.

The scatter plot of Th/K versus K (Fig. 2) shows considerable dispersion within and between the two sites. This dispersion suggests differences in paleoclimate conditions and depositional environments. Notably, dark shale deposits in Site 2, which contain organic matter and fossils, have very high Th/K ratios (high Th and low K), distinct from all other compositional units examined. The use of Th/K (and Th/U) as proxies for clay composition is notional and warrants further investigation using data from other instruments deployed in the field study (UV/VIS/IR + XRD) and/or laboratory studies of representative samples. Trace minerals associated with clays, such as phosphates, may account for much of the observed variation. Nevertheless, the apparent sensitivity of the elemental signatures to sedimentary processes should allow us to include radioelements in hypotheses tables used by the rover to investigate geologic origins [4]. As such, integration of the GRS with the rover DAC could be considered for the 2022 field season.

Conclusions: We demonstrated detailed mapping of surface radioelement concentrations with a rover-

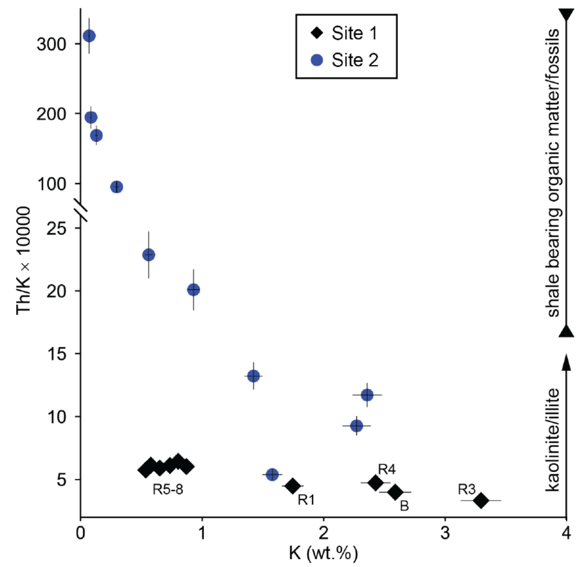

Figure 3. Th/K mass ratio versus K concentration reveals variations in the composition of sedimentary facies at the two field sites. Site 1 locations are shown in Fig. 2. Site 2 included light, tan, and red sedimentary rocks (low Th/K) and dark shale deposits containing organic matter and fossils (high Th/K). Dissimilar compositional trends between the sites suggest differences in the depositional environments. The Th/K ratio has been used in previous studies as a proxy for the composition of clay minerals as suggested by the right vertical arrow.

mounted GRS, complementing previous studies of sedimentary rocks via gamma-ray borehole/outcrop measurements. The elemental signatures are potentially sensitive to paleoclimate and sedimentation processes. Strong differentiation of organic-bearing shales from other sedimentary rocks was observed. Use of elemental signatures to characterize phyllosilicate-rich sediments could be extended to studies of Mars as well as water-rich bodies like Ceres that have surfaces rich in aqueous alteration products and organic matter. Additional empirical studies of radioelements in analogous hydrothermal systems would augment geochemical modeling used to interpret remote sensing data.

Acknowledgments: This work was funded by NASA through the SSERVI (NNH16ZDA001N) and DDAP (Grant #80NSSC20K1153) programs. We thank the Babbitt Ranches and the Hopi Tribe for permitting and supporting work on their lands.

References: [1] Prettyman T. H. *et al.* (2015), *Icarus, 259*, 39-52. [2] Ruffell A., and Worden R. (2000), *Palaeogeogr. Palaeoclimatol. Palaeoecol., 155*, 3, 265-283. [3] McLennan S. M. *et al.* (2019), *Annual Review of Earth and Planetary Sciences, 47*, 1, 91-118. [4] Dobrea E. N. (2022), *this meeting*. [5] Prettyman T. H. *et al.* (2020), *LPS LI*, #2570. [6] Prettyman T. H. *et al.* (2011), *Space Science Reviews, 163*, 1, 371-459. [7] Cabrol N. A. *et al.* (2007), *Journal of Geophysical Research: Biogeosciences, 112*, G4. [8] http://data.azgs.az.gov/geologic-map-of-arizona/.